Distribution and frequency of debris flows triggered by atmospheric rivers, Fraser Canyon, British Columbia

by

Kyra Baird

Thesis Submitted in Partial Fulfillment of the
Requirements for the Degree of
Physical Geography

in the
School of Environmental Science
Faculty of Environment

SIMON FRASER UNIVERSITY
Spring 2024

Declaration of Committee

Name:	**Kyra Baird**
Degree:	**Bachelor of Science (Geoscience)**
Title:	**Distribution and frequency of debris flows triggered by atmospheric rivers, Fraser Canyon, British Columbia**
Committee:	**Jeremy Venditti** Supervisor Professor, Environmental Science
	Julia Carr Supervisor Post-doctoral Researcher, Environmental Science

Abstract

Debris flows, common in mountainous terrain worldwide, are often primarily attributed to intense precipitation events, leading to rapid downslope transferals of sediment from hillslopes to channels and affecting fluvial processes. In southwestern British Columbia, atmospheric rivers are expected to become more intense and frequent, leading to an increase in debris flows. Despite this increase, the public and governing authorities lack awareness of these hazards. To enrich our understanding of these hazards, this research aims to investigate the impact of debris flows triggered by atmospheric rivers along the lower Fraser Canyon through satellite imagery and historical air photo analysis. The spatial distribution, frequency, and geomorphic changes caused by these events are examined, with a focus on the formation of Tikwalus Rapid. The slopes and areas between affected and stable tributary basins are compared to identify distinct characteristics of basins prone to these hazards. The findings enhance our understanding of landslide risks and their potential impacts on river systems.

Keywords: Debris flow; atmospheric river; Tikwalus Rapid; Fraser River

Acknowledgements

I could not have successfully completed this work without the exceptional support provided by my supervisors, for which I am incredibly grateful. I express extensive gratitude to Dr. Jeremy Venditti for his belief in my research capabilities and profound guidance throughout this project. Similarly, Dr. Julia Carr has played a crucial role in building my confidence to conduct research by offering constant support and encouragement. I feel fortunate to have had the opportunity to work alongside such passionate, dedicated, and supportive scientists at the River Dynamics Laboratory at Simon Fraser University who inspired me to push myself academically. I would like to extend my gratitude to Dr. Aaron Steelquist and Dr. Erin Seagren for sparking my interest in landslide research. I am incredibly grateful for the enthusiasm and support of Dr. Micheal Church for assisting in obtaining the air photos used in this research. LIDAR data used in this work was kindly contributed by the Hakai Institute. I am also deeply appreciative of my family and close friends for showing unwavering support and interest in my research. This project would not have been possible without the constant support from such a large, inspiring group of people.

I reside and study on the unceded traditional territories of the Kwantlen (q̓ʷɑ:ṅƛ̓əṅ), Katzie (q̓iċəy̓), Matsqui (Máthxwi), Semiahmoo (Se'mya'me), Musqueam (xʷməθkʷəy̓əm), Squamish (Sḵwx̱wú7mesh Úxwumixw), Tsleil-Waututh (sə̓liḷwətaʔɬ), and Kwikwetlem (kʷikʷəƛ̓əm) Nations. Data used in this research was collected on Nlaka’pamux (Nɬeʔkepmx Tmíxʷ) traditional territory. Throughout this research, I have gained a better understanding of the environmental and cultural significance of the Fraser River and surrounding lands. As I continue my career in Geoscience, I am committed to further developing my knowledge and actively integrating indigenous perspectives into my work to show my appreciation and honour towards the communities.

Lastly, I would like to recognize the generous funding provided by a Natural Science and Engineering Research Council Discovery Grant in addition to a British Columbia Salmon Restoration and Innovation Fund Grant to Dr. Jeremy Venditti.

Table of Contents

List of Tables

List of Figures

Chapter 1.

Introduction

Extensive rainfall is considered a common trigger for hillslope failure (Fan et al., 2020; Lee, 2017), particularly in regions that experience short-duration intense rainfall events, such as southwestern British Columbia where atmospheric rivers presently account for 33% of the total annual precipitation (Sharma & Déry, 2020). It has been argued that changes in regional-scale climate will result in more intense and frequent rainfall events and cause an increase the frequency of landslides in British Columbia (Sobie, 2020). As a result, the frequency of debris flows is expected to increase by 30% by the latter half of the 21st century (Gariano & Guzzetti, 2016; Jakob & Lambert, 2009; Sobie, 2020). While landslide hazards are expected to become more prevalent in British Columbia and other mountainous regions, both the public and governing authorities generally lack adequate awareness of areas vulnerable to landslide formation and the severity of impacts that may result from these failure events (Petschko et al., 2014).

On November 14th and 15th of 2021, two consecutive atmospheric rivers impacted southwestern British Columbia, causing extreme rainfall that reached over 200% of normal levels for the month (Sepúlveda et al., 2023). This event triggered a series of landslides along the Fraser River, causing extensive infrastructure damage and flooding that subsequently drove the province of British Columbia to declare a state of emergency. These landslides also posed an ecohazard to the Fraser River salmon by obstructing migration through the river and affecting populations in future spawning cycles (Evenden, 2004; Jackson, 1950; Venditti, 2024). When considering the storm average water vapour transport, the well understood variable typically used to characterize the intensity of an atmospheric river, the 2021 event corresponds to a 1 in 3.2-year event (Gillett et al., 2022). However, when considering only events with westerly oriented axes, where stronger water vapour is channeled into the eastern portion of the lower Fraser Valley, its significance elevates to a 1 in 11.8-year occurrence (Gillett et al., 2022). This is indicative that the orientation of atmospheric rivers have a large influence on their impact to specific regions.

The idea that an increase in the frequency and intensity of precipitation events will lead to an increase in landslide frequency does not consider the role of sediment

production and rock weathering in producing landslide debris. Forecasting the future occurrences of landslides is more reliant on evaluating the local terrain attributes associated with previous events (Montgomery et al., 2009; Petschko et al., 2014). By examining the distribution and frequency of debris flow events along with the distinct attributes of their respective basins, a more comprehensive understanding of their causative factors may be constructed. This aids in predicting potential future occurrences and enhances our knowledge on the contribution of these events to the geomorphic evolution of the Fraser River.

Beyond the immediate need to better understand how a shifting climate may impact landslide frequency, understanding the physical mechanisms of debris flow triggering along rivers contributes to our understanding of how river systems are organized. Within the canyons of large rivers, debris flows originating from steep tributary basins deliver coarse sediment to the mainstem channel, contributing to the cascade of sediment through the river (Fuller et al., 2016; Harvey, 2001; Webb et al., 1989). Understanding the behaviour and impacts of debris flows originating in hillslope tributaries on river incision is crucial for understanding sediment transport dynamics and hydraulic controls in bedrock river systems. For example, tributary inputs prone to landslides are responsible for the overall channel morphology, including the formation of fan-eddy complexes and rapids which alter flow dynamics (Finnegan et al., 2019; Larsen et al., 2004; Webb et al., 1989). The creation and modification of rapids are primarily influenced by the frequency and magnitude of debris flows from tributaries and the range of discharges in the mainstem (Larsen et al., 2004). While the interaction between the mainstem channel and tributary debris flows plays a significant role in shaping river morphology, the specific attributes of debris flows capable of blocking flow in the mainstem channel remain poorly understood (Finnegan et al., 2019; Larsen et al., 2004).

Here, I examine the locations of debris flows formed during the November 2021 atmospheric river event along the lower Fraser Canyon and determine the frequency of similar events in history using high resolution satellite imagery and historical air photos. The frequency of events are then compared to precipitation records to explore whether precipitation was a key causative factor in their occurrence. Beyond examining the distribution and frequency of failure events, I conduct a preliminary investigation into characteristics among three types of basins during the 2021 atmospheric river event: those that experienced failure events without affecting flow through the Fraser River,

those with failure events that created a sustained rapid on the Fraser River, and those that did not experience any failure events. To better understand the characteristics of debris flows capable of blocking flow through the Fraser River, I measure the topography and quantify the grain size distribution at the identified debris flow location which experienced the formation of a sustained rapid. This analysis allows for a more comprehensive understanding of the potential risk of future atmospheric rivers triggering landslides and forming hydraulic barriers on the Fraser River.

Chapter 2.

Methods

2.1 Study Area

The Fraser River and its tributaries cover approximately one third of British Columbia, draining approximately 232,000 km^2 of the province (Martins et al., 2011; Venditti & Church, 2014). The river stretches roughly 1,375 km from its source at Mount Robson to the Pacific Ocean at the Strait of Georgia in Vancouver, making it the longest river in British Columbia (Venditti & Church, 2014). The Fraser River itself was formed by mountain uplift during the Neogene and glaciation during the Pleistocene with tributaries consisting of till deposits reworked through postglacial erosion and recent mass-wasting events (Wright et al., 2022).The study area encompasses tributary basins surrounding a stretch of the Fraser River spanning approximately 86 km from Yale to Lytton (figure 1). This stretch is the southernmost section of the Fraser River Canyon, a 375 km bedrock influenced reach of the Fraser River between Yale and Soda Creek. While climate within this region varies, the study area experiences a warm-summer humid continental climate with a significant amount of rainfall throughout the year. Flow within the Fraser River is dominated by precipitation runoff and snowmelt from surrounding mountains, where its highest flows coincide with high snowmelt in the late spring to early summer, from May to June. At Hope, where the river flow outputs from the Fraser Canyon, the mean annual flow is roughly 2,730 m^3/s, with a mean annual peak flood flow of 8,665 m^3/s (Rennie et al., 2018).

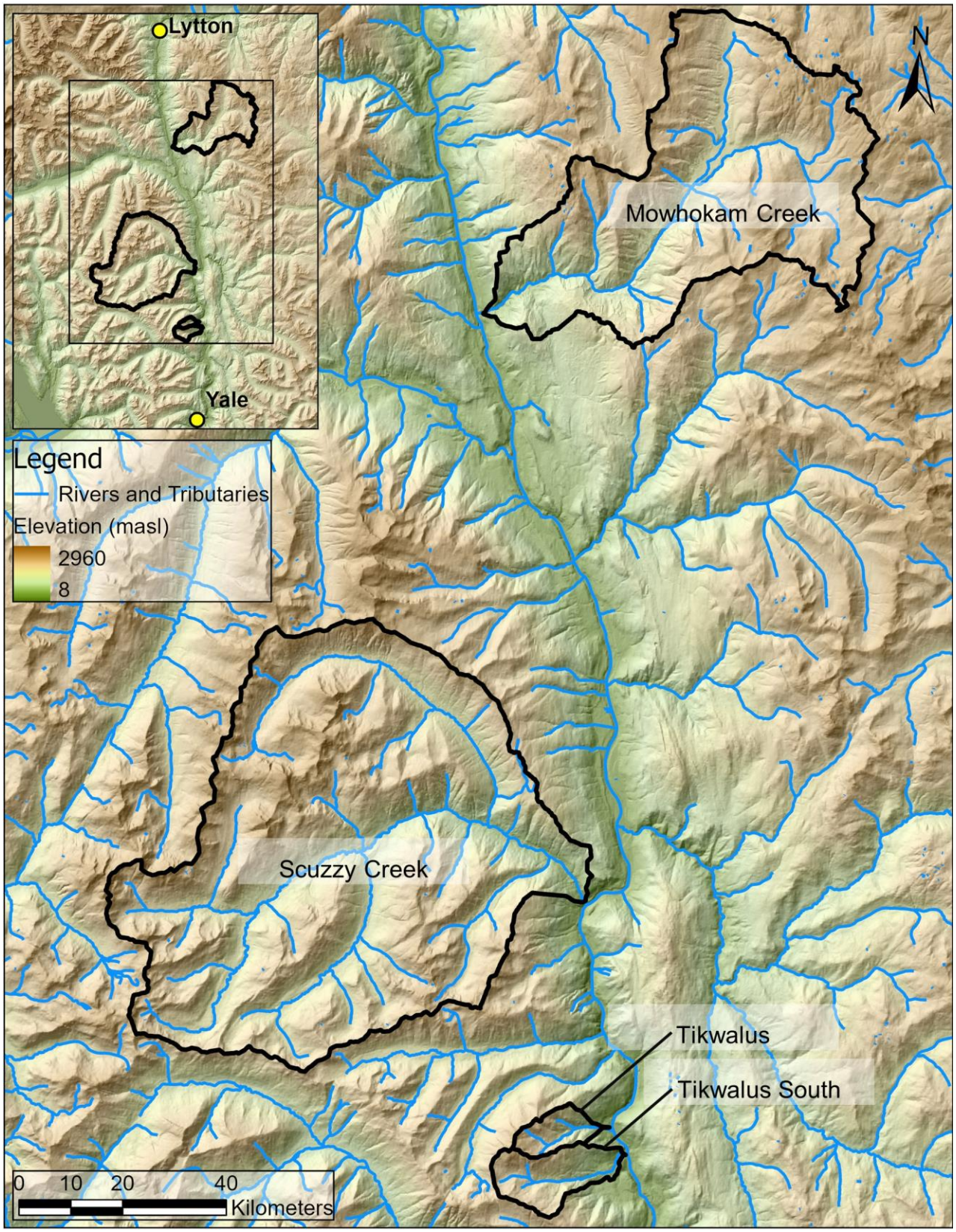

Figure 1. Map of the study area (top left) with the four identified basins which experienced debris flows attributed to the 2021 atmospheric river event (Mowhokam Creek, Scuzzy Creek, Tikwalus, and Tikwalus South) labelled on a smaller scale.

2.2 Satellite Imagery and Air Photo Analysis

To identify geomorphic changes from the 2021 atmospheric river event, I investigated Planet Labs Inc. (n.d.) satellite imagery from summer months in both 2021 and 2022 for evidence of mass wasting, such as newly exposed sediment, sediment accumulation in tributary channels, and vegetation cover degradation. A failure frequency analysis was then conducted using repeat satellite imagery (Planet Labs Inc., n.d.; table 1) from 2009 to 2021 to investigate any prior evidence of mass wasting at the identified debris flow sites to assess the timing of previous events and their impacts on the morphology of the Fraser River. To ensure optimal observation, satellite imagery was filtered to images captured during the summer months of each consecutive year and were selected based on parameters that best matched a Fraser River discharge of roughly 3,500 m^3/s (Government of Canada, 2024b) and minimal cloud cover. Uniformity of discharge values was imperative to accurately assess the impact of events on the mainstem channel morphology through sediment transport and debris fan deposition. The timing of each identified failure event was refined (table 2) using the Planet Labs Inc. explorer tool to analyze satellite imagery for landscape changes. This process was heavily reliant on the availability and clarity of imagery, where refining the timing of failure events proved particularly challenging during winter months due to prolonged periods of extensive cloud cover.

Table 1. Satellite imagery observed during the first order failure event frequency assessment for (a) Tikwalus, (b) Scuzzy Creek, (c) Mowhokam Creek, and (d) Tikwalus South. Recorded dates indicate the Planet Labs Inc. (n.d.) satellite imagery date observed for each location, and Fraser River discharge values are from the Hope gauge station (Water Survey of Canada Gauge 08MF005).

a)

Tikwalus	
Date	Fraser River Discharge (m^3/s)
30-08-2022	2,990
24-08-2021	2,330
27-08-2020	3,200
15-08-2019	3,150
06-08-2018	3,110
26-07-2017	3,200
11-08-2016	2,960
19-07-2015	3,280
17-08-2014	2,830
27-07-2013	3,720
12-08-2012	4,470
08-09-2011	2,460
18-08-2010	2,540
26-07-2009	3,930

b)

Scuzzy Creek	
Date	Fraser River Discharge (m^3/s)
30-08-2022	2,990
29-08-2021	2,040
26-08-2020	3,320
28-08-2019	2,820
27-08-2018	1,980
26-08-2017	2,000
24-08-2016	2,360
05-09-2015	2,070
24-08-2014	2,700
01-09-2013	2,210
12-08-2012	4,470
08-09-2011	2,460
18-08-2010	2,540
26-07-2009	3,930

c)

Mowhokam Creek	
Date	Fraser River Discharge (m^3/s)
30-08-2022	2,990
29-08-2021	2,040
26-08-2020	3,320
28-08-2019	2,820
05-09-2018	1,800
26-08-2017	2,000
13-09-2016	2,620
05-09-2015	2,070
04-09-2014	2,370
10-09-2013	2,170
13-09-2012	1,980
08-09-2011	2,460
02-09-2010	2,010
21-07-2009	3,930

d)

Tikwalus South	
Date	Fraser River Discharge (m^3/s)
30-08-2022	2,990
02-09-2021	1,820
26-08-2020	3,320
28-08-2019	2,820
17-08-2018	2,690
01-09-2017	1,870
30-08-2016	2,170
05-09-2015	2,070
23-08-2014	2,830
10-09-2013	2,170
13-09-2012	1,980
08-09-2011	2,460
18-08-2010	2,540
26-07-2009	3,930

Table 2. Dates of satellite imagery analyzed through the Planet Labs Inc. explorer tool for each of the identified debris flow locations. Start date and end date indicate, respectively, the start and end of the refined failure interval for each failure event observation.

Location	Start Date	End Date
Tikwalus	08-09-2011	19-05-2012
Scuzzy Creek	08-09-2011	12-05-2012
Tikwalus	05-07-2013	15-07-2013
Tikwalus	23-10-2015	29-03-2016
Tikwalus	06-09-2018	26-09-2018
Tikwalus	01-11-2021	09-03-2022
Tikwalus South	01-11-2022	09-03-2022
Mowhokam Creek	19-10-2021	08-03-2022
Scuzzy Creek	31-10-2021	27-01-2022

The location that experienced a 2021 debris flow event which had an affect on flow through the Fraser River, Tikwalus, was investigated for earlier failure events before 2009. To conduct this assessment, I analyzed all accessible historical air photos from the University of British Columbia Geographic Information Centre spanning from 1947 to 2003 (table 3), to identify evidence of failure events. To facilitate direct observation of landscape changes over time, physical historical images were scanned and digitized for manual georeferencing in GIS. Prominent features in the center of images, such as distinct bends in tributaries or large boulders, were aligned to minimize the distortion of images. Georeferenced images were then analyzed for the same debris flow indicators as described in the preceding process.

Table 3. Air photos observed during failure event frequency assessment for Tikwalus prior to 2009. Recorded dates indicate the air photo date observed for the Tikwalus basin, and Fraser River discharge values are from the Hope gauge station (Water Survey of Canada Gauge 08MF005).

Date	Fraser River Discharge (m^3/s)
30-06-1947	5,720
20-06-1948	4,250
20-08-1951	2,730
06-05-1952	3,110
14-05-1954	3,650
11-08-1961	3,230
16-09-1965	2,010
24-08-1966	3,170
06-05-1969	3,820
15-07-1973	4,980
07-07-1978	4,930
10-08-1979	2,720
04-08-1983	4,250
25-09-1991	1,890
04-08-1995	4,100
23-08-1996	3,430
19-07-1997	8,290
14-08-2002	2,980
30-08-2003	1,920

2.3 Comparison of Failure Events with Precipitation Data

To explore the influence of precipitation on landslide events, the refined timing of each event observed in satellite imagery from 2009 to 2023 was compared to precipitation data from the two nearest weather stations upstream and downstream of the study area at, Lytton and Hope, respectively (Government of Canada, 2024a). A time series of total daily precipitation from the two stations was generated and the constrained landslide occurrence intervals were plotted on the timeline. This allowed for a direct comparison between the specific landslide events and precipitation data for their respective failure time intervals.

2.4 Basin Characteristics Exploration

I analyzed tributary basin characteristics within the study area by delineating each basin using the watershed tool in GIS to calculate their respective areas. Subsequently, topographic slope across the study area was derived from a LIDAR

Digital Elevation Model, and zonal statistics were computed for the individual delineated basins to obtain the mean slope angle of each. These values were then plotted against the respective areas of basins to uncover potential disparities in characteristics between basins that experienced debris flows and those that remained stable.

2.5 Field Investigation

On August 9, 2023, I conducted a field investigation at Tikwalus, the site impacted by a debris flow during the November 2021 atmospheric river event that resulted in the formation of a sustained rapid on the Fraser River. The purpose was to assess sediment loading in both the tributary channel and debris fan formed on the mainstem channel. Quantification of sediment loading in the tributary channel and debris fan involved a cm-scale UAV photogrammetric survey using a DJI Mavic 3 Pro flown by Dr. Julia Carr. On August 9, 2023, multiple flights covered approximately the lower 1.5 km of the tributary channel leading to the mainstem, flying at altitudes ranging between 8 and 40 m above the channel (Carr et al., 2023). Each flight overlapped with the previous by at least 50 m and consisted of overlapping flight lines to ensure sufficient coverage of the terrain.

Data from these flights was processed using Agisoft Metashape 1.5.2 to generate 3D dense point clouds and a 7.2 cm resolution orthoimage of the tributary channel and debris fan. To evaluate sediment cover within the tributary channel and debris fan, the short axis of grains in plan-view on the orthoimage were manually measured in GIS. A systematic random sampling method was employed by overlaying a 4 m by 4 m grid onto the orthoimage where each grain located at grid line intersections was measured. These grain size measurements were used to create a grain size distribution that necessitated a comprehensive analysis of the coarse particle size distribution for both the main tributary channel and debris fan. This was achieved by determining the D16, D50, and D84 grain size values for the two locations and comparing the percent composition of grain sizes (i.e. gravels, cobbles, and boulders).

Chapter 3.

Results

3.1 History of Failure Events

Debris flows triggered by the two consecutive atmospheric rivers in November of 2021 were observed in four locations across the lower 86 km of the Fraser Canyon at Tikwalus, Scuzzy Creek, Mowhokam Creek, and in the basin 1.3 km south of Tikwalus, referred to as Tikwalus South. Satellite imagery from August 24th, 2021, and August 30th, 2022, revealed no significant changes to the terrain of other tributary basins within the study area, indicating that these were the only basins that displayed evidence of debris flows during this period. Frequency analysis of the four identified basins conducted from 2009 to before the 2021 atmospheric river event indicates that two of the locations experienced prior mass wasting events, while the terrain of the other two remained stable (figure 2). Tikwalus experienced many hillslope failures, distinct from debris flows, whereas Scuzzy Creek appears to have only experienced a single minor mass wasting event, akin to a debris flow, prior to November 2021. Meanwhile, Mowhokam Creek and Tikwalus South appear to have no evidence of prior significant mass wasting events.

Figure 2. Time series of failure event observations at the four identified basins. Each coloured diamond represent an observation of change at the site (landsliding, sediment loading, sediment evacuation), with all four sites having observations of debris flows during the 2021 atmospheric river event. Grey circles represent dates with imagery at the site but no observed change.

Many mass wasting events occurred at Tikwalus. Observed in historical air photos, the first evident failure within the Tikwalus tributary basin occurred on the hillslopes alongside newly constructed roadways between August 10th, 1979, and August 4th, 1983, due to disturbances to the natural landscape. Mass wasting on the natural hillslopes is evidenced by a scar forming on the hillslope between September 8, 2011, and May 19th, 2012. Shortly following this initial failure, a small southern scar forms between July 5th, 2013, and July 15th, 2013, merging with the main mass body of the pre-existing failure. This hillslope failed once again between October 23rd, 2015, and March 29th, 2016, where the failure created a small northern scar and the failed debris joined the pathway of previous failures on the terrain. Between September 6th, 2018, and September 26th, 2018, the original terrain separating the first scar formed and the small southern scar fails, contributing to the accumulation of debris from the previous failures. The last failure event observed in satellite imagery for this location took place between November 1st, 2021, and March 9th, 2022. Helicopter crews that flew through the Fraser Canyon in the few days immediately following the atmospheric river event on November 14th and 15th, 2021 observed debris flow evidence and a hydraulic rapid barrier on the Fraser River as a result of the event. This evidence supports the inference that the debris flow was a result of the atmospheric river event. Satellite imagery from August 30th, 2022, shows that the primary tributary channel expanded in width, on average, by 30 m due to deposition of debris, with the most significant change in channel width, approximately 50 m, occurring in the lower section of the primary tributary channel. Sediment loading in the tributary channels of this basin appears to be relatively patchy, where some sections of the channels show high concentrations of sediment deposition while others show minimal change in sediment cover. The imagery also reveals the formation of a persistent debris fan on the mainstem channel, disrupting river flow and leading to the formation of a hydraulic barrier on the Fraser River, known as Tikwalus Rapid. This sequence of failure events and the resulting geomorphic changes to the landscape are evident in figure 3, which shows a timeline of satellite imagery that documents the landscape evolution of Tikwalus.

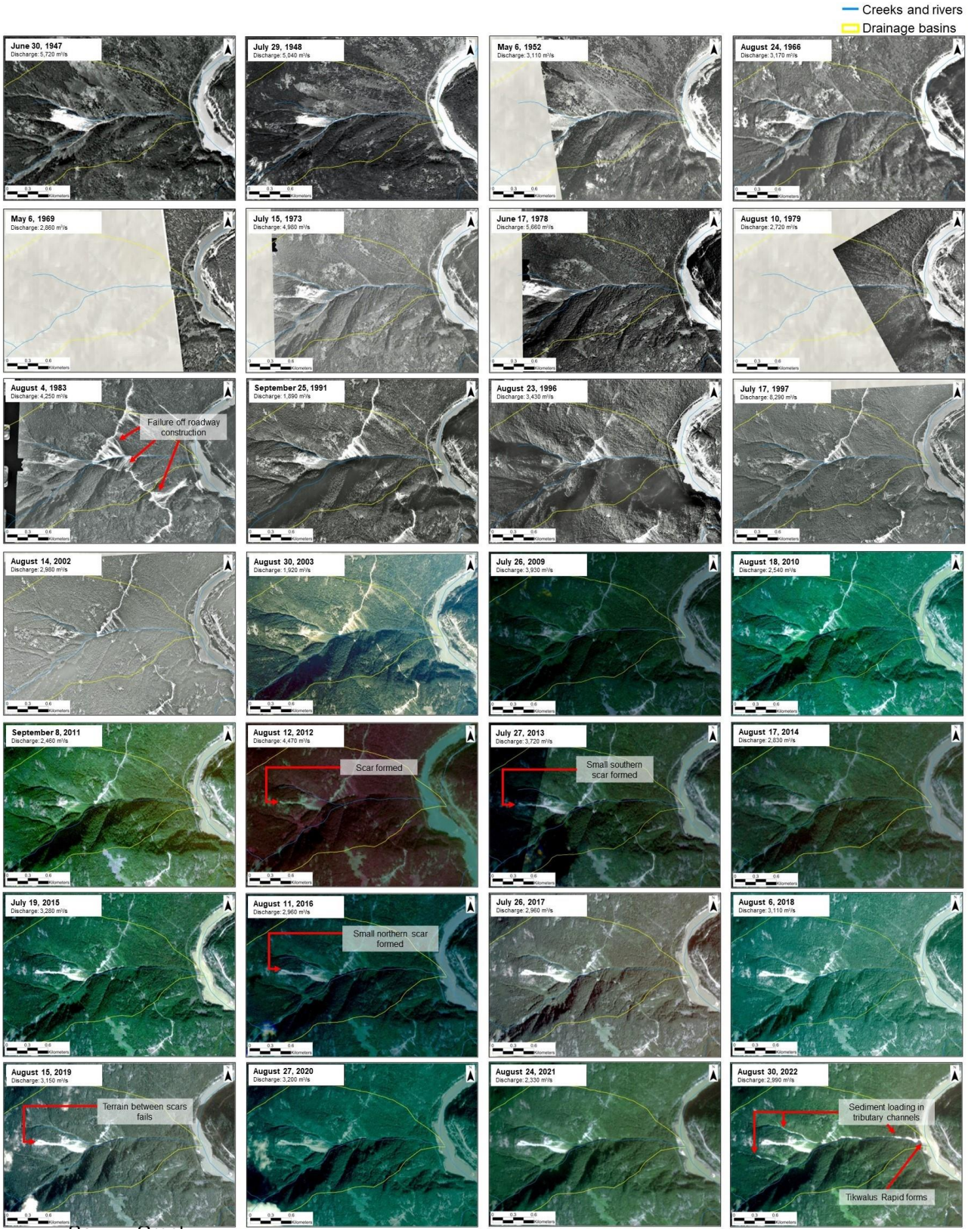

Figure 3. Time series of the Tikwalus basin located ~19 km North of Yale at 49°43'48"N, 121°26'04"W, illustrating landscape change as a result of mass wasting processes and hillslope failures. Selected satellite imagery from July 24, 2009 to August 30, 2022 are not representative of the most confined available images as minimal cloud cover and similar Fraser River discharge values were prioritized to provide the most accurate and optimal illustration of landscape changes. Imagery from June 30, 1947 to July 24, 2009 are the only available historical air photos covering the basin and therefore were not selected based on any prioritization.

Scuzzy Creek experienced a minor mass wasting event between September 8th, 2011, and May 12th, 2012, resulting in the formation of an alluvial fan with a maximum width of approximately 140 m that merges with the primary tributary channel. This location also experienced a debris flow which we attribute to the 2021 atmospheric river. As a result of the atmospheric river event, a significant amount of sediment loading in the basin's tributaries is evident in satellite imagery between October 31st, 2021 and January 27th, 2022. The primary tributary channel experiences the formation of braided sections where the channel expands by up to 60 m in width. The alluvial fan formed during the last noted failure event within this basin that disseminated over previous years has also been re-established during this event. Figure 4 shows the evolution of the tributaries within the Scuzzy Creek basin, resulting from the two identified failure events.

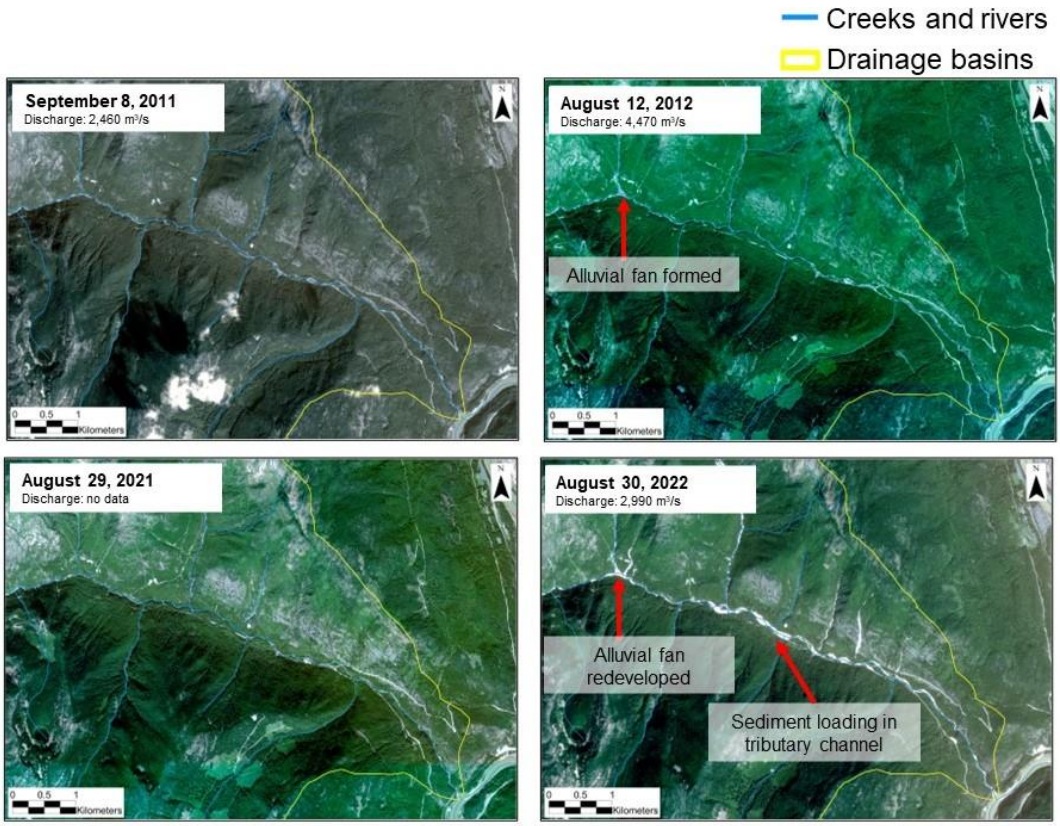

Figure 4. Time series of the Scuzzy Creek basin located ~28 km North of Yale at 49°48'48"N, 121°27'23"W, illustrating landscape change as a result of mass wasting processes. Selected satellite imagery are not representative of the most confined available images as minimal cloud cover and similar Fraser River discharge values were prioritized to provide the most accurate and optimal illustration of landscape changes.

The two other identified locations with debris flows attributed to the November 2021 atmospheric rivers are Mowhokam Creek and Tikwalus South. As a result, these locations experienced significant sediment loading in their primary tributary channels, evidenced by channel width expansion apparent between satellite imagery taken August 29th, 2021, and August 30th, 2022. In the Mowhokam Creek basin (figure 5a), sediment loading caused the primary tributary channel to expand by up to approximately 110 m. Figure 5b shows the formation of two scars on the hillslopes alongside a preexisting roadcut in the Tikwalus South basin. Sediment loading in the Tikwalus South tributary caused the channel to expand by up to 40 m. Apart from the 2021 debris flow observations, shown in figure 5, these two locations show no evidence of previous mass wasting events.

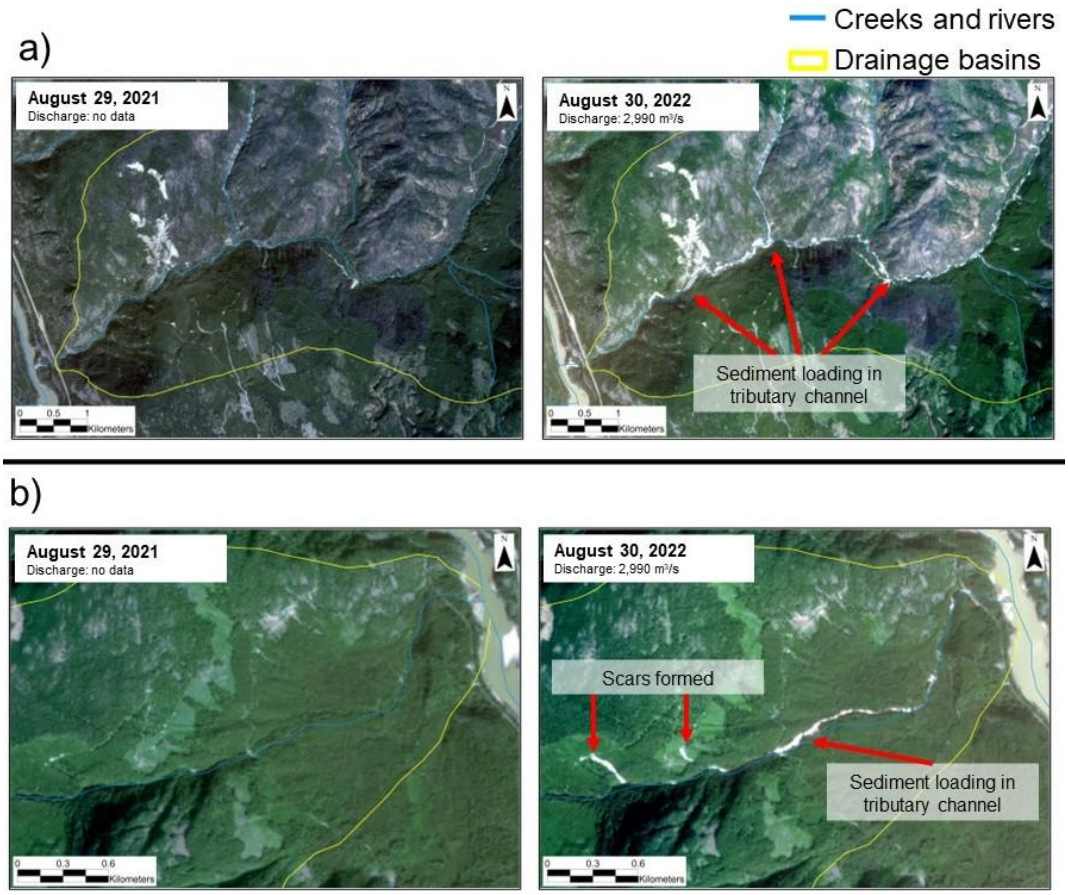

Figure 5. (a) Time series of the Mowhokam Creek basin located ~53 km North of Yale at 50°02'27"N, 121°30'41"W, illustrating landscape change as a result of debris flow attributed to the 2021 atmospheric river event. (b) Time series of the Tikwalus South basin located ~18 km North of Yale and ~1.3 km South of the Tikwalus basin at 49°43'07"N, 121°25'39"W, illustrating landscape change as a result of debris flow attributed to the 2021 atmospheric river event. Selected satellite imagery are not representative of the most confined available images as minimal cloud cover and similar Fraser River discharge values were prioritized to provide the most accurate and optimal illustration of landscape changes.

3.2 Relationship Between Failure Events and Precipitation

After aligning the constrained landslide occurrence intervals with the precipitation time series from 2009 to 2023 at Hope and Lytton (Government of Canada, 2024a; figure 6), it became evident that days with higher total precipitation levels within a year typically coincided with the constrained failure intervals. However, there are also numerous days with comparable precipitation levels that do not align with the identified failure intervals. A notable exception is observed on November 14th, 2021, during the atmospheric river event where precipitation levels at Hope were approximately double the second highest precipitation record in the timeline, coinciding with debris flow events at all four locations. This observation is not consistent with Lytton precipitation data. While the Lytton weather station reported a total precipitation of 29 mm for the day, multiple other days throughout the timeline experienced significantly higher precipitation levels where failure events were not evident within the four identified active basins.

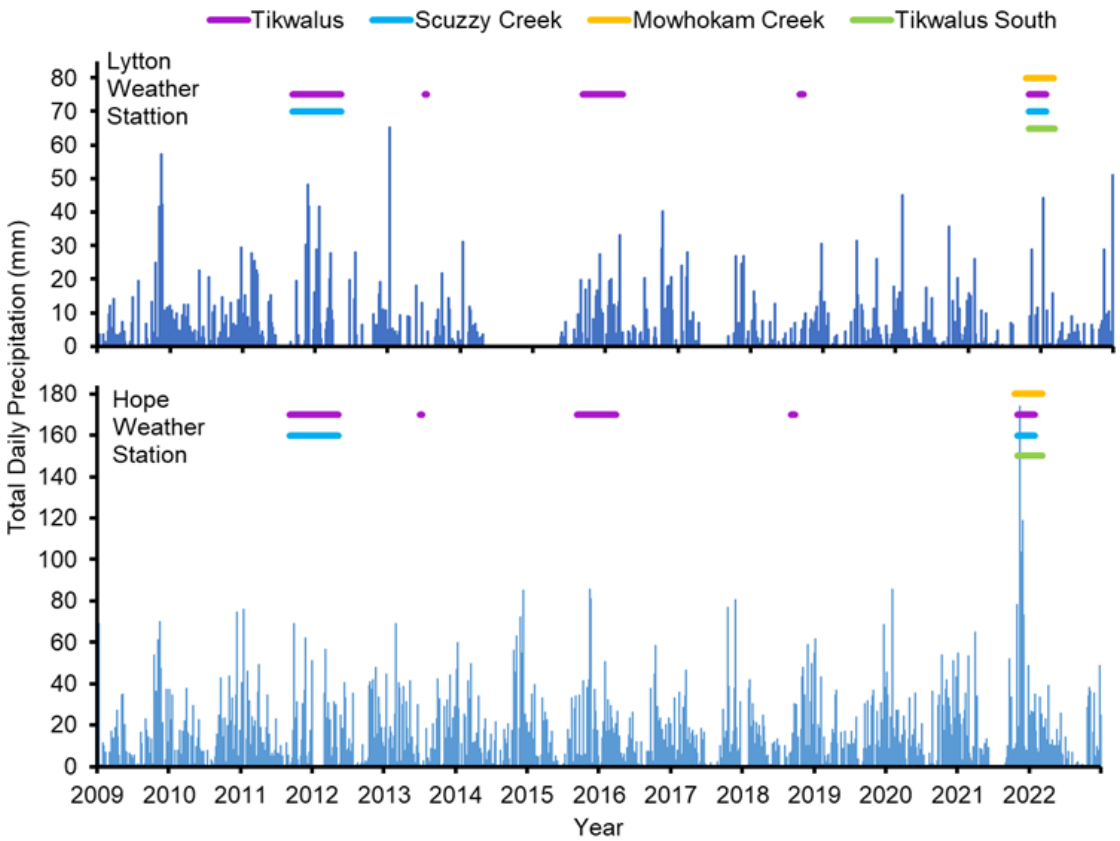

Figure 6. Failure event intervals defined by available satellite imagery for the four identified basins (bars coloured by site) aligned with a time series of the total daily precipitation measured at Hope (January 1, 2009-December 31, 2012 data from Hope AUT, January 1-July 31, 2012 data from Hope A, and August 1, 2012-December 31, 2022 data from Hope Airport) and Lytton (January 1, 2009-July 17, 2013 data from Lytton 2, and August 22, 2013-December 31, 2022 data from Lytton A) weather stations.

3.3 Basin Characteristics

Based on the comparison of basin area and mean slope (figure 7), there appears to be no significant differences between the four basins which experienced debris flows during the 2021 atmospheric river and those that remained stable. The data shows no clear trends of mean slope angle or area that differentiate the basins which experienced debris flows from those that did not; however, it is evident that Tikwalus, the 2021 debris flow location with a sustained impact on the mainstem channel, exhibits the highest mean slope angle (33.4˚) among all basins within the study area. It should also be considered that Tikwalus, with a drainage area of approximately 4.65 km^2, ranks in the lower 40% of basins.

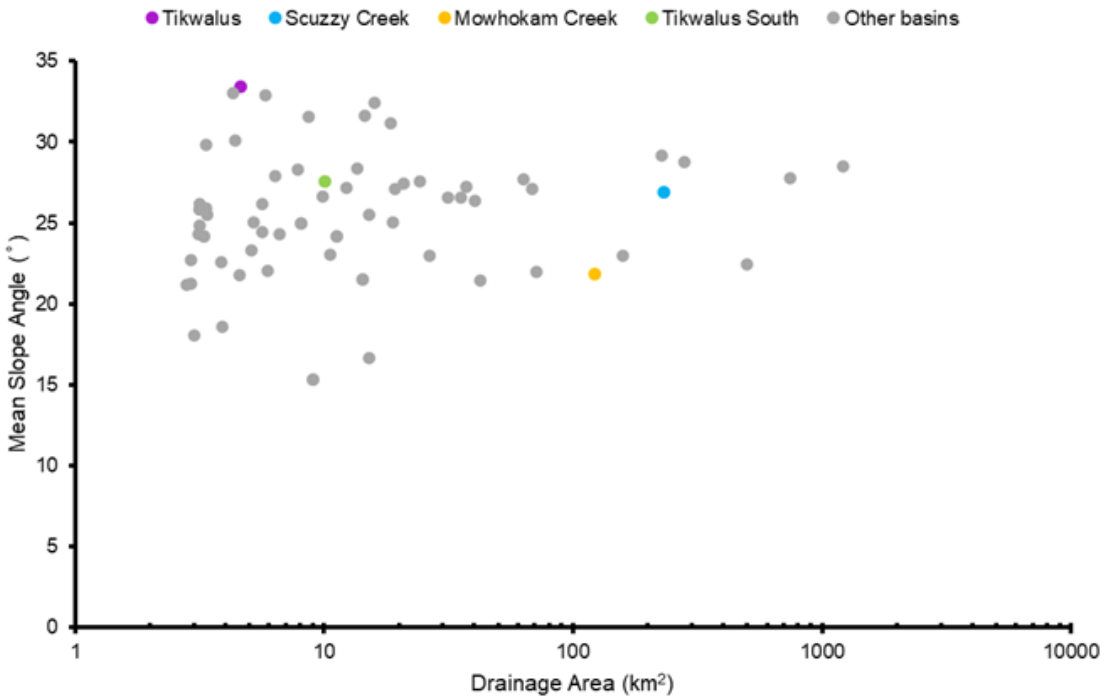

Figure 7. Comparison between drainage area and mean slope angle for the 77 basins within the study area. The identified debris flow basins are indicated as a respective colour for easy identification on the scatterplot, whereas basins which did not experience debris flows are indicated by grey.

3.4 Morphology and Grain Size Distribution at Tikwalus

Field investigations of the tributary channel and debris fan at Tikwalus revealed distinct features that were not identified in air photo and satellite imagery analysis of the basin. A sequence of five small waterfalls were discovered approximately 1.2 km up the main tributary channel from the Fraser River, totaling a relief of approximately 200m and spanning a total horizontal distance of about 300 m. The adjacent channel hillslopes surrounding the tributary channel exhibited extensive erosion, with channel bank materials consisting of a high proportion of fine-grained material interspersed with larger sized grains. Grain sizes ranging from cobbles to very large boulders predominantly covered the tributary channel and debris fan on the Fraser River. However, the grain size distribution observed at Tikwalus exhibited slight variation between its tributary channel and debris fan (figure 8). While the median size (D_{50}) for the tributary channel and debris fan were similar, respectively, 25.1 cm and 26.1 cm, there are disparities in the 16th (D_{16}) and 84th (D_{84}) percentiles of the distribution of the two locations. The D_{16} value of the tributary channel was 10.7 cm, whereas the value for the debris fan was 13.7 cm. The D_{84} value of the tributary channel is 68.7 cm, whereas the debris fan has a D_{84} value of 51.1 cm. Particles within the tributary channel comprise a higher proportion of grains less than the resolving limit of 7.2 cm, accounting for 4% of the total distribution, compared to the debris fan percentage of 2%. This assessment of grains below the resolving limit (7.2 cm) cannot be used to quantify the presence of fine grains as the orthoimage resolution is much greater than the threshold between fine and coarse grain sizes (4.75 mm). As a result, fine grained sediments fall below the detection limit in the imagery and are not accounted for by this method, indicating the percentage of grains less than 7.2 cm are representative of the amount of gravels within the debris flow deposit. The proportion of cobbles and boulders within both the tributary channel and debris fan do not vary significantly. In the tributary channel, cobbles account for 53% of the grains, while boulders make up 42% of the total, whereas across the debris fan, cobbles constitute 56% of the grains, with boulders comprising 42% of the total.

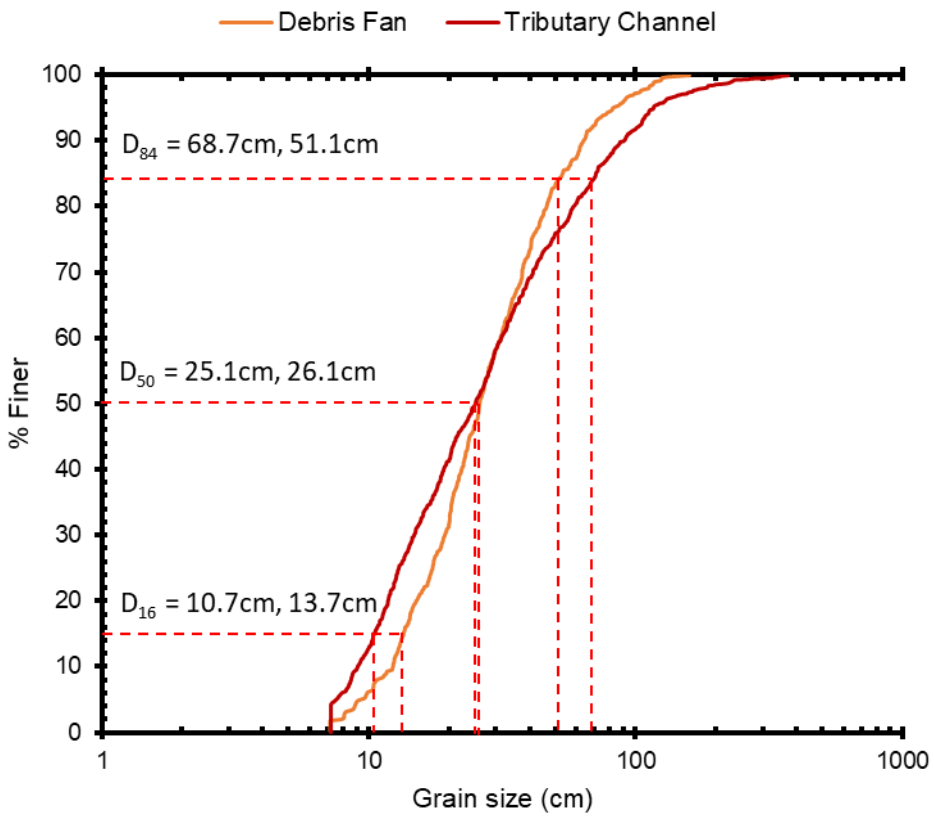

Figure 8. Grain size distribution of the debris fan and Tikwalus tributary channel obtained through an orthoimage derived from the UAV photogrammetric survey on August 9th, 2023. The resolving limit in this distribution is 7.2 cm, constrained by the resolution of the orthoimage used in the survey.

Chapter 4.

Discussion

The observed variation in sediment cover throughout the Tikwalus tributary is likely a result of differences in vegetation density surrounding the channel, which creates a patchy appearance in certain areas due to larger shadows. Sections of the channel that are surrounded by a greater vegetation density will appear to have a reduced sediment cover due to the formation of a shadow in the imagery. Shadowing effects in satellite imagery and air photos may obscure or underrepresent the actual volume of sediment cover, presenting a challenge in accurately assessing the magnitude of the debris flow event. (Steger et al., 2021). While this is particularly evident in the Tikwalus tributary, this challenge is likely prevalent in all observed satellite images and air photos, potentially resulting in an overall underrepresentation of debris flow observations across tributary basins within the study area. The concept of shadows creating an effect of the appearance of sediment accumulation in tributary channels was confirmed for the Tikwalus tributary basin during field investigation as sediment cover did not appear patchy and was primarily consistent throughout the channel. This shadow effect may have also obscured other debris flows formed during the 2021 atmospheric river event, preventing their detection in this study.

It is crucial to consider the different climactic zones of Hope and Lytton when comparing precipitation data with the timing of identified landslide events. Hope, situated within the same climactic zone as the observed debris flow sites, exhibits a temperate climate that experiences a significant amount of rainfall throughout the year, even during the driest months. Meanwhile, located just 100 km North of Hope, Lytton has a semi-arid climate which experiences significantly less precipitation in comparison. The discrepancy in precipitation data between Hope and Lytton, which accounts for the inconsistent results in correlating landslide occurrences with rainfall during the 2021 atmospheric river event, may be attributed to the distinct climates of the two cities. While the high precipitation experienced at Hope during the 2021 atmospheric river event aligned with debris flows at the four identified locations, drier conditions experienced at Lytton during the event underscore the complexity of climate and landslide dynamics. It must also be considered that the westerly orientation of the 2021 atmospheric river likely had a

significant influence on the distribution of precipitation experienced during the event as Hope experienced stronger water vapour and ultimately greater precipitation levels (Gillett et al., 2022).

While debris flows in four locations attributed to the 2021 atmospheric river event were evidently triggered by the significant rainfall experienced, the relation between debris flow occurrence and precipitation may be more intricate than solely explained by precipitation data. When comparing the constrained landslide occurrence intervals with precipitation data, it becomes apparent that the frequency of precipitation events with landslide triggering potential is much higher than the actual number of landslides observed. In addition, there are no distinct reasons (drainage area and tributary morphology) that explain the onset of these events. This suggests that the occurrence of landslides may be significantly dependent on an interplay of longer-term stochastic processes governing sediment accumulation in the tributary channels. These processes include factors such as hillslope weathering (Anderson et al., 2002; Rengers, Kean, et al., 2020), sediment production rates (Anderson et al., 2002; Bennett et al., 2014), the development of fractures (Montgomery et al., 2009), and local variables specific to each location, such as soil depth (Dietrich et al., 1995), and vegetation cover (Rengers, McGuire, et al., 2020). While the immediate trigger for these debris flows may be the intense rainfall experienced during the atmospheric river event, the buildup of sediment in these channels may predispose them to failure.

Notably, only one of the four debris flow locations, Tikwalus, impacted the mainstem, locally altering flow conditions and forming a rapid that continues to influence the Fraser River across seasonal discharge levels. One potential factor contributing to this distinct impact is the composition and volume of sediment delivered to the mainstem channel during the debris flow event. It is expected that the Tikwalus debris flow transported a larger volume of sediment to the mainstem channel, or that the sediment grains were significantly coarser than those at other debris flow sites, helping them resist suspension in the river flow (Li et al., 2024). This may be a result of the basin constituting the highest slope or the most active hillslopes amongst debris flow basins, leading to a greater accumulation of readily available sediment for transport in its tributary channel. Additionally, the impact on the mainstem is significantly influenced by the local channel characteristics at each site, including slope, width, and depth, which determines whether the river at that specific location is capable of mobilizing the input of sediment (Finnegan

et al., 2019). A larger product of channel slope, width, and depth means the mainstem channel is capable of mobilizing larger grain sizes, contributing to the cascade of sediment through the river that alters channel morphology downstream (Finnegan et al., 2019; Fuller et al., 2016; Harvey, 2001; Webb et al., 1989). Considering these factors, the combination of channel characteristics (slope, width, and depth) at the output of Tikwalus basin may be lower compared to the output of other debris flow basins, resulting in the mainstem at Tikwalus not being able to mobilize as large grain sizes as it can at other sites.

Conclusion

Satellite imagery and historical air photos were used to investigate the distribution and frequency of mass wasting events along the lower Fraser Canyon. The timing of failure events was compared to precipitation data to analyze whether rainfall was a key causative factor in their occurrence. Local basin attributes were compared between basins that experienced debris flows during the 2021 atmospheric river event with and without a sustained affect on the flow through the Fraser River and basins that did not show evidence of failure events as a result of the atmospheric river. These analyses allowed for a better understanding of the dynamics behind the failure events where findings demonstrated that the relationship between precipitation is much more complex than previously thought. Many comparable precipitation events to the 2021 atmospheric river occurred over the observed time period yet did not coincide with the timing of failure events. In addition, there were no distinctions in the areas and slopes of basins which experienced debris flows in 2021 from those that remained stable. However, the one identified basin that experienced a debris flow with a sustained disruption to flow through the Fraser River had the steepest mean slope throughout its basin and the most active hillslopes, with multiple previous failure events. These findings suggest that the failure events are likely more influenced by a combination of longer-term stochastic processes. Further research is needed to examine specific terrain attributes of the three types of basins analyzed (those that experienced failure events without affecting flow through the Fraser River, those with failure events that created a sustained rapid on the Fraser River, and those that did not experience any failure events) to better understand reasoning behind why basins reacted differently to the atmospheric river event. Additionally, conducting field investigations at other debris flow sites to obtain grain size distributions of debris flows that did not significantly impact river flow, and comparing these with the distribution from the debris flow that created the persistent rapid on the Fraser River (Tikwalus Rapid), would provide insight into the behaviours and mechanisms of debris flows which are capable of obstructing river flow.

References

Anderson, S. P., Dietrich, W. E., & Brimhall, G. H., Jr. (2002). Weathering profiles, mass-balance analysis, and rates of solute loss: Linkages between weathering and erosion in a small, steep catchment. *GSA Bulletin*, *114*(9), 1143–1158. https://doi.org/10.1130/0016-7606(2002)114<1143:WPMBAA>2.0.CO;2

Bennett, G. L., Molnar, P., McArdell, B. W., & Burlando, P. (2014). A probabilistic sediment cascade model of sediment transfer in the Illgraben. *Water Resources Research*, *50*(2), 1225–1244. https://doi.org/10.1002/2013WR013806

Carr, J. C., DiBiase, R. A., Yeh, E.-C., Fisher, D. M., & Kirby, E. (2023). Rock properties and sediment caliber govern bedrock river morphology across the Taiwan Central Range. *Science Advances*, *9*(46), eadg6794. https://doi.org/10.1126/sciadv.adg6794

Dietrich, W. E., Reiss, R., Hsu, M., & Montgomery, D. R. (1995). A process-based model for colluvial soil depth and shallow landsliding using digital elevation data. *Hydrological Processes*, *9*(3–4), 383–400. https://doi.org/10.1002/hyp.3360090311

Evenden, M. (2004). Social and environmental change at Hells Gate, British Columbia. *Journal of Historical Geography*, *30*(1), 130–153. https://doi.org/10.1016/S0305-7488(02)00104-4

Fan, L., Lehmann, P., Zheng, C., & Or, D. (2020). Rainfall intensity temporal patterns affect shallow landslide triggering and hazard evolution. *Geophysical Research Letters*, *47*(1). https://doi.org/10.1029/2019GL085994

Finnegan, N. J., Broudy, K. N., Nereson, A. L., Roering, J. J., Handwerger, A. L., & Bennett, G. (2019). River channel width controls blocking by slow-moving

landslides in California's Franciscan mélange. *Earth Surface Dynamics*, *7*(3), 879–894. https://doi.org/10.5194/esurf-7-879-2019

Fuller, I. C., Riedler, R. A., Bell, R., Marden, M., & Glade, T. (2016). Landslide-driven erosion and slope–channel coupling in steep, forested terrain, Ruahine Ranges, New Zealand, 1946–2011. *CATENA*, *142*, 252–268. https://doi.org/10.1016/j.catena.2016.03.019

Gariano, S. L., & Guzzetti, F. (2016). Landslides in a changing climate. *Earth-Science Reviews*, *162*, 227–252. https://doi.org/10.1016/j.earscirev.2016.08.011

Gillett, N. P., Cannon, A. J., Malinina, E., Schnorbus, M., Anslow, F., Sun, Q., Kirchmeier-Young, M., Zwiers, F., Seiler, C., Zhang, X., Flato, G., Wan, H., Li, G., & Castellan, A. (2022). Human influence on the 2021 British Columbia floods. *Weather and Climate Extremes*, *36*, 100441. https://doi.org/10.1016/j.wace.2022.100441

Government of Canada. (2024a). Climate. https://climate.weather.gc.ca/historical_data/search_historic_data_e.html

Government of Canada. (2024b). Water Level and Flow - Environment Canada. https://wateroffice.ec.gc.ca/report/real_time_e.html?stn=08MF005

Harvey, A. M. (2001). Coupling between hillslopes and channels in upland fluvial systems: Implications for landscape sensitivity, illustrated from the Howgill Fells, northwest England. *CATENA*, *42*(2), 225–250. https://doi.org/10.1016/S0341-8162(00)00139-9

Jackson, R. I. (1950). *Variations in flow patterns at Hell's Gate and their relationships to the migration of sockeye salmon*. International Pacific Salmon Fisheries Commission.

Jakob, M., & Lambert, S. (2009). Climate change effects on landslides along the southwest coast of British Columbia. *Geomorphology*, *107*(3), 275–284. https://doi.org/10.1016/j.geomorph.2008.12.009

Larsen, I. J., Schmidt, J. C., & Martin, J. A. (2004). Debris-fan reworking during low-magnitude floods in the Green River canyons of the eastern Uinta Mountains, Colorado and Utah. *Geology*, *32*(4), 309–312. https://doi.org/10.1130/G20235.1

Lee, C.-T. (2017). Landslide trends under extreme climate events. *Terrestrial, Atmospheric and Oceanic Sciences*, *28*(1), 33–42. https://doi.org/10.3319/TAO.2016.05.28.01(CCA)

Li, C.-J., Hu, Y.-X., Fan, G., Zhu, Q.-Y., Liu, D.-R., & Zhou, J.-W. (2024). Exploring debris flow deposit morphology in river valleys: Insights from physical modeling experiments. *Engineering Geology*, *332*, 107465. https://doi.org/10.1016/j.enggeo.2024.107465

Martins, E. G., Hinch, S. G., Patterson, D. A., Hague, M. J., Cooke, S. J., Miller, K. M., Lapointe, M. F., English, K. K., & Farrell, A. P. (2011). Effects of river temperature and climate warming on stock-specific survival of adult migrating Fraser River sockeye salmon (Oncorhynchus nerka). *Global Change Biology*, *17*(1), 99–114. https://doi.org/10.1111/j.1365-2486.2010.02241.x

Montgomery, D. R., Schmidt, K. M., Dietrich, W. E., & McKean, J. (2009). Instrumental record of debris flow initiation during natural rainfall: Implications for modeling slope stability. *Journal of Geophysical Research: Earth Surface*, *114*(F1). https://doi.org/10.1029/2008JF001078

Petschko, H., Brenning, A., Bell, R., Goetz, J., & Glade, T. (2014). Assessing the quality of landslide susceptibility maps – case study Lower Austria. *Natural Hazards and Earth System Sciences*, *14*(1), 95–118. https://doi.org/10.5194/nhess-14-95-2014

Planet Labs Inc. (n.d.). Planet Explorer. https://www.planet.com/explorer/

Rengers, F. K., Kean, J. W., Reitman, N. G., Smith, J. B., Coe, J. A., & McGuire, L. A. (2020). The Influence of Frost Weathering on Debris Flow Sediment Supply in an Alpine Basin. *Journal of Geophysical Research: Earth Surface*, *125*(2), e2019JF005369. https://doi.org/10.1029/2019JF005369

Rengers, F. K., McGuire, L. A., Oakley, N. S., Kean, J. W., Staley, D. M., & Tang, H. (2020). Landslides after wildfire: Initiation, magnitude, and mobility. *Landslides*, *17*(11), 2631–2641. https://doi.org/10.1007/s10346-020-01506-3

Rennie, C. D., Church, M., & Venditti, J. G. (2018). Rock Control of River Geometry: The Fraser Canyons. *Journal of Geophysical Research: Earth Surface*, *123*(8), 1860–1878. https://doi.org/10.1029/2017JF004458

Sepúlveda, S. A., Ward, B. C., Cosman, S. B., & Jacobs, R. (2023). Preliminary investigations of ground failures triggered during the mid-November 2021 atmospheric river event along the southwestern British Columbia highway corridors. *Canadian Geotechnical Journal*, *60*(4), 580–586. https://doi.org/10.1139/cgj-2022-0093

Sharma, A. R., & Déry, S. J. (2020). Contribution of atmospheric rivers to annual, seasonal, and extreme precipitation across British Columbia and southeastern Alaska. *Journal of Geophysical Research: Atmospheres*, *125*(9), e2019JD031823. https://doi.org/10.1029/2019JD031823

Sobie, S. R. (2020). Future changes in precipitation-caused landslide frequency in British Columbia. *Climatic Change*, *162*(2), 465–484. https://doi.org/10.1007/s10584-020-02788-1

Steger, S., Mair, V., Kofler, C., Pittore, M., Zebisch, M., & Schneiderbauer, S. (2021). Correlation does not imply geomorphic causation in data-driven landslide

susceptibility modelling – Benefits of exploring landslide data collection effects. *Science of The Total Environment*, *776*, 145935. https://doi.org/10.1016/j.scitotenv.2021.145935

Venditti, J. G., & Church, M. (2014). Morphology and controls on the position of a gravel-sand transition: Fraser River, British Columbia: Gravel-Sand Transition. *Journal of Geophysical Research: Earth Surface*, *119*(9), 1959–1976. https://doi.org/10.1002/2014JF003147

Webb, R. H., Pringle, P. T., & Rink, G. R. (1989). Debris flows from tributaries of the Colorado River, Grand Canyon National Park, Arizona. *Professional Paper*, Article 1492. https://doi.org/10.3133/pp1492

Wright, M., Venditti, J. G., Li, T., Hurson, M., Chartrand, S., Rennie, C., & Church, M. (2022). Covariation in width and depth in bedrock rivers. *Earth Surface Processes and Landforms*, *47*(6), 1570–1582. https://doi.org/10.1002/esp.5335